INTERNATIONAL ATOMIC ENERGY AGENCY
UNITED NATIONS EDUCATIONAL, SCIENTIFIC AND CULTURAL ORGANIZATION

INTERNATIONAL CENTRE FOR THEORETICAL PHYSICS
34100 TRIESTE (ITALY) - P.O.B. 586 - MIRAMARE - STRADA COSTIERA 11 - TELEPHONES: 224281/2/3/4/5/6
CABLE: CENTRATOM - TELEX 460392-1

SMR/100 - 50

WINTER COLLEGE ON LASERS, ATOMIC AND MOLECULAR PHYSICS

(24 January - 25 March 1983)

Influence of the Inversion Depletion in the Active Medium on the Evolution of Ultrashort Pulses in Passively Mode-Locked Solid-State Lasers.

B. WILHELMI

Friedrich-Schiller-Universität Jena
Sektion Physik
Max-Wien-Platz, 1
69 Jena
Dem. Rep. Germany

Influence of the Inversion Depletion in the Active Medium on the Evolution of Ultrashort Pulses in Passively Mode-Locked Solid-State Lasers

J. Herrmann, F. Weidner and *B. Wilhelmi*

Dept. of Physics, University of Jena, DDR-69 Jena, German Democratic Republic

Received 20 October 1978/Accepted 21 June 1979

Abstract. An analytical treatment of the ultrashort-pulse generation in a solid-state laser is given taking into account gain saturation. The probability for the breakdown of the picosecond-pulse evolution caused by the amplification depletion is calculated. The influence of the active medium saturation on the satellite-pulse probability is investigated. Both probabilities characterize the mode-locking behaviour of the laser system and are calculated for various laser parameters to find an optimum laser regime.

PACS: 42.55

The generation of ultrashort pulses in passively mode-locked solid-state lasers has been investigated by several authors [1–14]. In the fluctuation model mode-locking is explained by the selection and progressive enhancement of a single fluctuation peak from the initial multimode emission intensity of the laser. Analytical treatments of this process were presented in [1–7]. In these papers the pulse evolution is divided in a linear, a nonlinear and a giant pulse stage. Their analysis is founded on the assumption that the pulse selection by the saturable absorber is completed in the nonlinear absorption stage before any appreciable depletion of the population inversion in the active medium occurs. The results obtained by using this assumption provide a qualitative understanding of the pulse generation process. But experimental investigations [8–10] showed that under certain conditions the pulse formation can be influenced by the inversion depletion in the active medium. In these experiments the existence of two thresholds was observed. Free-running oscillation arises when the pumping energy reaches the laser threshold (first threshold). A train of ultrashort pulses only appears when the pumping energy exceeds the mode-locking threshold (second threshold). The existence of the second threshold is attributed to the reduction of the population inversion during the nonlinear stage.

Hitherto theoretical investigations concerning the influence of gain saturation were carried out founded on computer simulations [11–14]. Lariontsev and Serkin [11] investigated the optimum cavity length for a maximum contrast of the ultrashort pulses. The existence of an optimum cavity length is connected with the nonlinear action of the active medium. In [11] a very simple model of the radiation field was used allowing only a qualitative discussion of the investigated effect. A computer simulation was also presented by Glenn [12]. From the results of his calculations Glenn concluded that by the influence of the amplification depletion the efficient single-pulse selection is enormously enhanced. But Glenn strongly overestimated the depletion of the population inversion by the laser radiation. In [Ref. 12, Eq. (19)] used in the computer calculations the cavity round-trip time has to be substituted by the pulse duration. Wilbrandt and Weber [13] investigated the second threshold and its probabilistic nature for a mode-locked Nd:YAG laser in more detail. In their calculations the authors used a slow saturable absorber (energy relaxation time long compared with the duration of the fluctuation peaks).

Such an absorber provides only a weak pulse selection and represents a disadvantageous approximation for the solid-state laser situation. More recently New [14] presented results of a computer calculation of the second threshold including the noise statistics in a realistic way for one set of Nd:YAG laser parameters.

In the present paper an analytical treatment of the picosecond-pulse generation in a passively mode-locked solid-state laser is given taking into account gain saturation. By the influence of the depletion of the population inversion in the active medium a critical intensity level relatively to the mean intensity exists at the end of the stage of linear amplification.

Fluctuation peaks with intensities above this critical level are amplified, the others are damped. From the existence of this critical level the probability for an early breakdown of the single-pulse evolution is calculated. In this case the laser system remains in a regime of free-running oscillation. Since this probability very sensitively depends on the pumping rate the second threshold for the pumping rate characterized by a low breakdown probability may be estimated. For fixed values of the pump rate and of the other laser parameters an optimum cavity length with a minimal probability of the breakdown exists. We give an approximated analytical expression of this optimum cavity length.

Besides the probability for the breakdown of the pulse formation the probability for the appearance of double pulses is another feature of a mode-locked laser system. With increasing pumping rate the double-pulse probability becomes larger, but the breakdown probability decreases. For good mode-locking both probabilities shall be small. Therefore an optimization of the laser system may be performed comparing both probabilities in dependence on the pumping rate and the cavity length.

1. Linear Stage of Pulse Evolution

The pulse evolution is described by the following basic equations [7]

$$\frac{\partial E_L(k,\omega-\omega_L)}{\partial k} = \frac{1}{2}E_L(k,\omega-\omega_L)\left[\frac{a(k)}{L(\omega-\omega_L)}-\gamma\right] + \frac{C}{L(\omega-\omega_L)}N(k,\omega-\omega_L) - \frac{1}{2}\varkappa\int_{-\infty}^{\infty}\frac{E_L(k,\tau)}{1+\mu|E_L(k,\tau)|^2}e^{-i(\omega-\omega_L)\tau}d\tau, \tag{1}$$

$$\frac{da(k)}{dk} = P-\beta a(k)\overline{|E_L(k)|^2}\,; \tag{2}$$

k is the number of cavity round-trips after exceeding the laser threshold.

$$E_L(k,\omega-\omega_L) = \int_{-\infty}^{\infty} d\tau \exp[-i(\omega-\omega_L)\tau]E_L(k,\tau)$$

is the Fourier transformed field strength. τ marks the time coordinate during a cavity round trip: $-U/2 \leqq \tau < U/2$, where U is the cavity round trip period. $\overline{|E_L(k)|^2}$ designates the time average over a cavity round trip:

$$\overline{|E_L(k)|^2} = \frac{1}{U}\int_{-U/2}^{+U/2} d\tau |E_L(k,\tau)|^2 .$$

In (1) a fluctuation force $N(k,\tau)$ was introduced. $N(k,\tau)$ represents a white Gaussian random noise process. $a(k) = 2\sigma^a L^a n^a(\varrho^a_{22}-\varrho^a_{11})$ is the gain per pass in the centre of the laser line. γ and $\varkappa = 2\sigma^b L^b n^b$ contain the constant cavity losses and the small signal absorption of the saturable absorber per pass, respectively.

The other abbreviations are

$$L(\omega-\omega_L) = 1 + 2i(\omega-\omega_L)/\Delta\omega^a,$$

$$C = -2i\hbar\sigma^a L^a n^a/\mu^a_{12},$$

$$\beta = (\varepsilon^a/\mu_0)^{1/2}\sigma^a U/\hbar\omega_L,$$

$$\mu = (\varepsilon^b/\mu_0)^{1/2}(2I^b_s)^{-1}.$$

I^b_s is the absorber saturation intensity, σ the absorption cross section, n the particle number density, L the length of the medium, ϱ_{ik} the density matrix elements, μ_{12} the matrix element of the dipole operator, ω_L the laser frequency, and $\Delta\omega^a = 2\pi\Delta\nu^a$ the spectral width of the homogeneously broadened laser line. The quantities referring to the active medium are denoted by the index a and those referring to the absorber by the index b.

P is the approximately constant and frequency-independent pumping rate per pass. For a ruby laser (three-level system), it is given by

$$P = U\sigma_p F_p(k=0)(a_{\max}-a_{Thr}),$$

for a Nd:glass laser (four-level system) by

$$P = U[\sigma_p F_p(k=0)a_{\max} - a_{Thr}/T^a_1],$$

with $a_{\max} = 2\sigma^a L^a n^a$ and $a_{Thr} = \varkappa+\gamma$. σ_p is the absorption cross-section for the pump radiation, F_p the pump photon flux density at laser threshold ($k=0$).

The pulse evolution starts with the exceeding of the laser threshold. At this point the amplification a_{Thr} just compensates the cavity losses ($a_{Thr} = \varkappa+\gamma$). Above threshold a period of linear behaviour of the absorption and amplification begins. The fluctuation force and the frequency dependence of the amplification expressed by $L(\omega-\omega_L)$ are taken into calculation. Because of the low intensity the population changes

caused by the laser radiation in the absorber and the active medium are negligible. Using these approximations the normalized field-strength correlation function is given by [7]

$$\chi(k,h) = \frac{\langle E_L(k,\tau)E^*_L(k,\tau+h)\rangle}{\langle|E_L(k,\tau)|^2\rangle} = \exp\left\{-2(\ln 2)\left(\frac{h}{T(k)}\right)^2\right\}, \tag{3}$$

where $T(k) = 2(\pi\Delta\nu^a)^{-1}\{2a_{Thr}k\ln 2\}^{1/2}$. The radiation field $E_L(k,\tau)$ can be treated as a narrow-band Gaussian noise process during the linear stage.

The statistical average of the intensity is [7]

$$\langle I(k)\rangle = \langle I_{Thr}\rangle\frac{eP k^2/2}{\sqrt{2Pa_{Thr}k}}. \tag{4}$$

I_{Thr} is the intensity at laser threshold. During the linear stage the statistical average corresponds to the time average over one cavity round-trip ($\langle I(k)\rangle = \overline{I(k)}$) [7]. The expressions (3) and (4) are valid for $k \gg 1$. The amplification increases linearly ($a = a_{Thr}+Pk$). Different from [1–7] we define the end of the linear stage by the condition

$$\sigma a_{Thr}\langle I(k_0)\rangle = P, \tag{5}$$

where $\sigma = \sigma^a U(\sigma^b T^b_1)^{-1}$. This means that the depletion of the population inversion in the active medium caused by the laser radiation becomes essential at $k = k_0$.

The intensity is normalized to the absorber saturation intensity $I^b_s = \hbar\omega_L(\sigma^b T^b_1)^{-1}$. Using (4) and (5) we find an approximate expression for the number of cavity round-trips in the linear stage

$$k_0 = \left\{\frac{2}{P}\ln\left(\frac{P}{\sigma a_{Thr}\langle I_{Thr}\rangle}\sqrt{2Pa_{Thr}}\cdot\sqrt{\frac{2}{P}\ln\frac{P}{\sigma a_{Thr}\langle I_{Thr}\rangle}}\right)\right\}^{1,2}. \tag{6}$$

For usual solid-state laser parameters the influence of the nonlinear absorption at $k = k_0$ is negligible.

2. The Effect of the Amplification Depletion During the Nonlinear Stage

Due to the natural mode selection the width of the fluctuation peaks increases proportional to $\sqrt{k}$ during the linear stage leading to a spectral narrowing of the radiation. Since the linear stage includes several thousands of cavity round-trips and the number of cavity round-trips between the end of the linear stage and the end of the pulse development is small compared with k_0, the frequency dependence of the amplification is negligible for $k > k_0$.

Supposing that the absorber energy relaxation time T^b_1 fulfils the relation $T^b_1 \ll T(k_0)$ the intensity dependence of the absorber losses is given by $\varkappa/(1+I)$. We devide the nonlinear stage into three parts. During the first part immediately after the linear stage the absorber losses may be expanded up to the first order of the intensity. At the end of the range of validity of this expansion (at $k = k_1$) the intensity I_1 of the highest fluctuation peak is in the order of $I_1(k_2) \approx 0.2$. During the second part of the nonlinear stage the peak intensity exceeds the absorber saturation intensity. Therefore, in this phase the exact form $\varkappa/(1+I)$ of the nonlinear absorption has to be taken into account. It will be shown that in these two parts of the nonlinear stage in ruby and Nd:glass laser systems the reduction of the amplification by the laser field is small compared to the threshold amplification a_{Thr}. This is not fulfilled for the Nd:YAG laser. The stimulated emission cross section of the Nd:YAG exceeds the cross sections the two other laser types by a factor 30 leading to a much faster depletion of the population inversion in the Nd:YAG system. Therefore, the following calculations are valid only for ruby and Nd:glass lasers.

In the first part of the nonlinear stage the small depletion of the population inversion may strongly affect the pulse evolution since the laser is working just above the threshold. The second part of the nonlinear stage is characterized by the action of the saturable absorber; the influence of the inversion depletion is negligible. Therefore, the probability of the breakdown of the picosecond pulse generation caused by the combined action of small population changes in the active medium and in the saturable absorber is essentially determined in the first part of the nonlinear stage, as will be shown later. In the third part of the nonlinear stage, which may be called giant pulse stage, the absorber is completely saturated. The pulse intensity increases very rapidly leading to a fast depletion of the population inversion. A train of picosecond pulses having pulse distances equal to the cavity round-trip time leaves the laser. The statistical properties of the radiation field do not change during this part of the pulse development (cf. [Ref. 7, Sect. 7]).

Using the approximations discussed above the first part of the nonlinear stage is described by the equations

$$\frac{\partial I(k,\tau)}{\partial k} = \tilde{a}(k)I(k,\tau)+\varkappa I^2(k,\tau), \tag{7}$$

$$\frac{d\tilde{a}(k)}{dk} = -\sigma a_{Thr}\overline{I(k)}, \tag{8}$$

where we introduced the excess amplification $\tilde{a} = a - a_{Thr}$ and used the relation $\tilde{a} \ll a_{Thr}$. With the

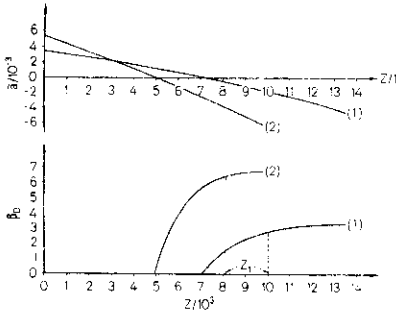

Fig. 1. Excess amplification $\tilde{a}$ and discrimination parameter β_D as a function of z for ruby laser and Nd:glass laser parameters. The parameter values are $U=6$ ns, $P=4\cdot10^{-7}$, $a_{Thr}=0.5$, $\varkappa=0.3$ for the ruby laser (curves 1) and $U=6$ ns, $P=10^{-6}$, $a_{Thr}=0.5$, $\varkappa=0.3$ for the Nd:glass laser (curves 2)

variable

$$z(k)=\int_{k_0}^{k} dk' \exp\left[\int_{k_0}^{k'} dk''\tilde{a}(k'')\right] \tag{9}$$

the solution of (7) may be written as

$$I(z,\tau)=\frac{I(k_0,\tau)\frac{dz}{dk}}{1-\varkappa I(k_0,\tau)z}. \tag{10}$$

The limit of validity of the solution (10) is characterized by the condition $I_1(k_1)\approx0.2$ for the highest fluctuation peak. At this limit the term $\varkappa I_1(k_0)z$ is in the order of unity. Since the averaged intensity of the highest fluctuation peak characterized by the condition $\bar{N}(\beta^{\max},U)=1$, cf. (21), exceeds the mean intensity $\overline{I(k_0)}$ at the end of the linear stage by a factor $\beta^{\max}$ in the order of five to ten, the averaged intensity $\overline{I(z)}$ can be calculated by expanding (10) up to the second order in z:

$$\overline{I(z)}=\frac{dz}{dk}\left[\overline{I(k_0)}+\varkappa z\overline{I^2(k_0)}+(\varkappa z)^2\overline{I^3(k_0)}\right]. \tag{11}$$

If $I(k_0,\tau)$ would be an exact stationary random process with the probability density

$$p(I)=\langle I(k_0)\rangle^{-1}\exp[-I/\langle I(k_0)\rangle]$$

the mean value $\langle I(z)\rangle$ would diverge. Since $I(k_0,\tau)$ is only defined in the time interval $-U/2\leqq\tau<+U/2$ the correspondence between the statistical and the time average is limited (cf. [Ref. 7, Sect. 5]). The main contribution to the average

$$\langle I^n(k_0)\rangle=\langle I(k_0)\rangle^{-1}\int_0^\infty dI\, I^n\exp[-I/\langle I(k_0)\rangle]$$

results from the region around $n\langle I(k_0)\rangle$. Therefore, the statistical average differs essentially from the time average over a cavity round trip for $n\gtrsim\beta^{\max}$. But up to $n=3$ both averages agree and we obtain $\overline{I^2(k_0)}=2\overline{I(k_0)}^2$ and $\overline{I^3(k_0)}=6\overline{I(k_0)}^3$. Putting (9) and (11) into (8) we obtain an equation for $z(k)$:

$$\frac{d^2}{dk^2}\ln\frac{dz}{dk}=-\sigma a_{Thr}\overline{I(k_0)}\frac{dz}{dk}\cdot[1+2\varkappa\overline{I(k_0)}z+6(\varkappa\overline{I(k_0)}z)^2]. \tag{12}$$

The initial conditions are $z(k_0)=0$, $dz/dk|_{k_0}=1$ and $d^2z/dk^2|_{k_0}=\tilde{a}(k_0)$. Equation (12) can be reduced to a first-order differential equation

$$\frac{dz}{dk}(z)=-\tfrac{1}{2}\sigma a_{Thr}\overline{I(k_0)}z^2\cdot[1+\tfrac{2}{3}\varkappa\overline{I(k_0)}z+(\varkappa\overline{I(k_0)}z)^2]+\tilde{a}(k_0)z+1. \tag{13}$$

Equation (13) may be solved by separation of the variables and decomposition into partial fractions. This solution of (13) is unnecessary because we need only dz/dk as a function of z in the following calculations.

If the excess amplification is reduced to values $\tilde{a}<0$ the first term in (7) becomes negative. The fluctuation peak for which the first term is dominant (that means $\partial I/\partial k<0$) is damped. If at a given moment the relation $\partial I/\partial k<0$ holds it remains valid for all later times too, and I goes to zero. The maximum condition $\partial I/\partial k=0$ marks the end of the amplification region of the fluctuation peak under consideration. From the definition of z it follows that $dz/dk>0$ is valid for all k. Therefore, the condition $\partial I/\partial k=0$ is equivalent to $\partial I/\partial z=0$. We consider the ensemble of fluctuation peaks at the end of the linear phase ($k=k_0$). Using the average $\overline{I(k_0)}$ as unit for the intensity the fluctuation peak intensity is described by the dimensionless factor $\beta=I(k_0,\tau)/\overline{I(k_0)}$. Combining (10) with the maximum condition $\partial I/\partial z=0$ we obtain

$$\beta_D(z)=-\frac{\tilde{a}(z)}{\varkappa\overline{I(k_0)}\left[\frac{dz}{dk}(z)-\tilde{a}(z)z\right]}. \tag{14}$$

This formula means that pulses with the intensity $\beta_D\overline{I(k_0)}$ at the end of the linear stage reach their maximum at the point z. $\tilde{a}(z)$ is given by $d/dz[dz/dk]$. Using (13) we find

$$\tilde{a}(z)=-\sigma a_{Thr}\overline{I(k_0)}z\{1+\varkappa\overline{I(k_0)}z+2[\varkappa\overline{I(k_0)}z]^2\}+\tilde{a}(k_0). \tag{15}$$

The functions $\tilde{a}(z)$ and $\beta_D(z)$ are depicted in Fig. 1 for ruby and Nd:glass laser parameters. In all numerical calculations of this paper we use the parameters

$\sigma^a=2.5\cdot10^{-20}\,\mathrm{cm}^2$, $\Delta\nu^a=3.3\cdot10^{11}$ Hz, $T_1^b=14$ ps, $\sigma^b=10^{-15}\,\mathrm{cm}^2$, $\langle I_{Thr}\rangle=10^{-1.2}$ for the ruby laser and $\sigma^a=3\cdot10^{-20}\,\mathrm{cm}^2$, $\Delta\nu^a=7\cdot10^{12}$ Hz, $T_1^b=8$ ps, $\sigma^b=5.7\cdot10^{-16}\,\mathrm{cm}^2$, $\langle I_{Thr}\rangle=10^{-1.2}$ for the Nd:glass laser. The other parameters are given in the figure caption in each case.

All pulses with $\beta>\beta_D$, lying above the curve $\beta_D(z)$, are amplified, the pulses with $\beta<\beta_D$ are discriminated. The function $\beta_D(z)$ reaches its maximum value $\beta_D^{\max}$ at $z=13{,}500$ (ruby laser) and $z=9800$ (Nd:glass laser), respectively, where $dz/dk(z)=0$.

However the validity of the approximations discussed at the beginning of this section ends at smaller z-values ($z=z_1$). At this point $z=z_1$ the intensity of the highest fluctuation peak is $I^{\max}(z_1)=0.2$. For the parameters used in Fig. 1 we find $z_1=10{,}030$ for the ruby laser and $z_1=8120$ for the Nd:glass laser. z_1 marks the end of the first part of the nonlinear stage ($k=k_1$). For $k>k_1$ the exact form $\varkappa/(1+I)$ of the absorber nonlinearity has to be taken into account providing higher absorber losses than the expansion of $\varkappa/(1+I)$ used in (7). By these higher losses the intensity increases slower than discribed by (7) leading to a slower depletion of the population inversion. Then the effect of the pulse discrimination will be weaker. The ascent of the exact curve $\beta_D(z)$ would be flatter for $z>z_1$ than the ascent of the curve in Fig. 1b and 2b. Since the variation of $\beta_D(z)$ in the range $z>z_1$ is small the maximum value $\beta_D^{\max}$ provided by (14) does not essentially differ from the maximum value of the curve $\beta_D(z)$ obtained by using the exact absorber losses. Independent on z_1 the maximum value $\beta_D^{\max}$ may be regarded as the upper limit of the pulse discrimination.

Using (14) and (5) the condition $dz/dk=0$ in (13) provides for $\beta_D^{\max}$ the relation

$$(\beta_D^{\max})^2+\frac{\sigma a_{Thr}\tilde{a}(k_0)}{\varkappa P}\beta_D^{\max}-\frac{(\sigma a_{Thr})^2}{2\varkappa^2 P}\cdot\left[1+\frac{2}{3\beta_D^{\max}}+\frac{1}{(\beta_D^{\max})^2}\right]=0. \tag{16}$$

For $\beta_D^{\max}\lesssim3$ higher-order correction terms in the square brackets have to be taken into calculation.

We compared the analytical result (16) with New's computer simulations [14]. New calculated 100 individual laser shots for one given set of Nd:YAG laser parameters. Using these parameters equation (16) provides $\beta_D^{\max}=3.76$. New found in his calculation $\beta_D^{\max}=4.05$. The probability of the breakdown of the pulse evolution (derived in the next section) is 23% for this parameters. New found that from 100 shots modelocking failed to occur in 20 cases. The results are in good correspondence though the approximations made to derive equation (16) are better fulfilled for the ruby and Nd:glass system than for the Nd:YAG laser.

3. Probability for the Breakdown of the Pulse Evolution

If none of the fluctuation peaks exceeds the level $\beta_D^{\max}$ at the end of the linear stage all peaks are discriminated and the pulse evolution breaks down. We may calculate the probability for the occurance of this event. The probability of the case that the amplitude A of a narrow-band noise process exceeds the level A_D during the time interval $(\tau,\tau+\Delta\tau)$ is given by [15]:

$$W_{\Delta\tau}^{ex}=\int_0^\infty d\dot{A}\int_{A_D-\dot{A}\Delta\tau}^{A_D} dA\, p_2(A,\dot{A}). \tag{17}$$

$p_2(A,\dot{A})$ is the joint probability density of the amplitude A and its time derivation $\dot{A}$. If $\Delta\tau$ is small enough this expression can be expanded up to the first power of $\Delta\tau$:

$$W_{\Delta\tau}^{ex}=\Delta\tau\int_0^\infty d\dot{A}\dot{A}\,p_2(A_D-\dot{A}\Delta\tau,\dot{A})=\bar{N}_{\Delta\tau}\Delta\tau. \tag{18}$$

The ratio of the number $\bar{N}$ of intervals $\Delta\tau$ during which the level A_D is exceeded to the total number $n(n\gg1)$ of intervals is equal to the probability $W_{\Delta\tau}^{ex}=\bar{N}_{\Delta\tau}\Delta\tau=\bar{N}/n$ that during an arbitrary chosen interval $\Delta\tau$ the event "A_D is exceeded" occurs. The observation time of the process is the cavity round-trip period $U=n\cdot\Delta\tau$. In the limit $\Delta\tau\to0$ we find

$$\bar{N}=U\int_0^\infty d\dot{A}\dot{A}\,p_2(A_D,\dot{A}). \tag{19}$$

Applying formula (19) to a narrow-band Gaussian noise process one obtains for the mean number of exceedings of the level $\beta\langle I\rangle$ during the time U the expression [16]:

$$\bar{N}(\beta,U)=U\sqrt{-\frac{\beta}{\pi}\frac{d^2}{dh^2}\chi(h)|_{h=0}}\,e^{-\beta} \tag{20}$$

$\chi(h)$ is the normalized field strength correlation function. Using (3) taken at $k=k_0$ we obtain

$$\bar{N}(\beta,U)=\frac{U}{T(K_0)}\sqrt{\frac{4\ln2}{2}}\beta e^{-\beta}. \tag{21}$$

The condition $\bar{N}(\beta^{\max},U)=1$ defines the averaged intensity of the highest fluctuation peak at $k=k_0$. Putting $\beta_D^{\max}$ into the expression (21) we obtain the mean number of exceedings of the level $\beta_D^{\max}$ at the end of the linear stage.

$W_{\Delta\tau}=1-W_{\Delta\tau}^{ex}$ is the probability that during one interval $\Delta\tau$ the level A_D is not exceeded. The probability that during all $n=U/\Delta\tau$ intervals the level A_D is not exceeded is $W_U=(W_{\Delta\tau})^n$. In the limit $\Delta\tau\to0$ we receive

$$W(\beta_D^{\max},U)=\exp[-\bar{N}(\beta_D^{\max},U)]. \tag{22}$$

This is the probability that the pulse evolution breaks down and no pulse train leaves the laser.

The breakdown probability shows an interesting dependence on the cavity length. At fixed laser parameters an optimum cavity round-trip time U_{opt} exists where the breakdown probability is minimal. We may derive an approximate analytical expression of the optimum cavity round-trip time and the corresponding breakdown probability. For solid-state laser parameters the term $(\beta_D^{max})^2$ may be neglected in (16). Since all other parameters are fixed equation (16) provides U as a function of β_D^{max}. In this calculation the dependence of the pumping rate P on the cavity round-trip time has to be regarded since $\delta = P/U$ is a constant (cf. Sect. 1). Using the function $U = U(\beta_D^{max})$ in (21) $\bar{N}(\beta_D^{max}, U)$ is given as a function of β_D^{max} alone

$$\bar{N}(\beta_D^{max}) = \Phi \frac{(\beta_D^{max})^3 \, e^{-\beta_D^{max}}}{\left[1 + \frac{2}{3\beta_D^{max}} + \frac{1}{(\beta_D^{max})^2}\right]^{5/2}}, \tag{23}$$

where Φ is a constant depending on the laser parameters. The maximum condition

$\frac{d\bar{N}(\beta_D^{max})}{d\beta_D^{max}} = 0$ provides the equation for $(\beta_D^{max})_{opt}$:

$$(\beta_D^{max})_{opt}^3 - \tfrac{7}{3}(\beta_D^{max})_{opt}^2 - \tfrac{8}{3}(\beta_D^{max})_{opt} - 8 = 0.$$

Its only real solution is $(\beta_D^{max})_{opt} = 3.659$ independent on the laser parameters. Putting this value into the functions $U = U(\beta_D^{max})$ and $\bar{N} = \bar{N}(\beta_D^{max})$ we receive

$$U_{opt} = 67.8\delta \left(\frac{\sigma^b T_1^b \varkappa}{\sigma^a a_{Thr}}\right)^2 \cdot \eta, \tag{24}$$

$$\bar{N}_{opt} = 10.10\delta^{3/2} \frac{\Delta\nu^a}{a_{Thr}^3} \left(\frac{\sigma^b T_1^b \varkappa}{\sigma^a}\right)^{5/2} \cdot \eta \tag{25}$$

with

$$\eta = \ln\left[4.83\delta^{3/2} \frac{\sqrt{\varkappa}}{a_{Thr}\langle I_{Thr}\rangle} \left(\frac{\sigma^b T_1^b}{\sigma^a}\right)^{3/2}\right] + \tfrac{1}{4} \ln \ln\left(\frac{\delta^{5/4} \sigma^b T_1^b}{\sigma^a \langle I_{Thr}\rangle} \sqrt{\frac{2}{a_{Thr}}}\right)$$

Putting $\bar{N}_{opt}$ into (22) we get the corresponding breakdown probability.

4. Estimation of the Double-Pulse Probability Taking into Account Gain Saturation

Besides the second threshold condition the probability of the appearance of satellite pulses is another feature of good mode-locking. In a model with constant gain during the nonlinear stage this probability was calculated by Demokan and Lindsay [5, 6]. In this section we want to investigate the influence of the amplification reduction on the double-pulse probability. At first we calculate the ratio of the two highest fluctuation peaks $X = I_1(k_1)/I_2(k_1)$ at the end of the first part of the nonlinear stage as a function of the intensity $I_1(k_1)$ of the highest peak and the ratio $Y = I_1(k_0)/I_2(k_0)$ at the end of the linear stage. Using the equations (10) and (13) we find

$$X = 1 + \frac{[1 + (s-1)I_1(k_1)](Y-1)}{1 - (g/\beta_1)}, \tag{26}$$

where $s = \varkappa/\tilde{a}(k_0) + 1$ and

$$g = \left[\frac{(s-1)I_1(k_1)}{1 + (s-1)I_1(k_1)}\right]^2 \frac{\sigma a_{Thr}}{2 \cdot \varkappa \tilde{a}(k_0)} \left(1 + \frac{2}{3\beta_1} + \frac{1}{(\beta_1)^2}\right).$$

Deriving (26) the relation

$$2\sigma a_{Thr}(s-1)I_1(k_1)[\varkappa\tilde{a}(k_0)]^{-1} \cdot [1 + (s-1)I_1(k_1)]^{-2}\beta_1^{-1} \ll 1$$

fulfilled for solid-state laser parameters was used.

β_1 denotes the intensity of the highest fluctuation peak at the end of the linear stage. It is a stochastic quantity. At the end of the first part of the nonlinear stage for ruby and Nd:glass laser parameters the relation $|\tilde{a}(k_1)| \ll a_{Thr}$ is valid (cf. Fig. 1). Also during the second part of the nonlinear stage the reduction of the population inversion is small for ruby and Nd:glass lasers. An estimation of the amplification depletion during this stage provides [7]

$$|\tilde{a}(k_2)| \approx \frac{2I_1(k_2)a_{Thr}\sigma^a T(k_2)}{\varkappa\sigma^b T_1^b} \ll a_{Thr}. \tag{27}$$

The intensity of the highest fluctuation peak $I_1(k_2)$ at the end of the second part of the nonlinear stage ($k = k_2$) is in the order of ten. We can conclude that for the highest fluctuation peaks during the second part of the nonlinear stage the term $\tilde{a}I$ in (7) is negligible. The equation

$$\frac{\partial I}{\partial k} = \frac{\varkappa I^2}{1 + I} \tag{28}$$

provides for the intensity ratio $Z = I_1(k_2)/I_2(k_2)$ of the two highest peaks at the end of the second part of the nonlinear stage

$$Z = X \exp\left[\frac{1}{I_1(k_1)}(X-1)\right]. \tag{29}$$

where the relation $I_{1,2}(k_2) \gg 1$ is used. $I_1(k_1)$ is the nonrandom limit of the first part of the nonlinear stage fitting equation (26) to (29). In our calculations we chose $I_1(k_1) = 0.2$.

In the giant pulse stage the amplification reduction has to be taken into consideration, but the absorber losses can be neglected. Therefore, the intensity ratio remains constant and the probability distribution function $F(Z)$ for double pulses can be determined using (26) and (29). Now we calculate $F(Z)$. At the end of the linear stage the field strength is normally distributed. According to [5] the bi-variable probability density function for the intensity of the highest (β_1) and second highest fluctuation peak (β_2) normalized to the mean intensity $I(k_0)$ is given by

$$p_2(\beta_1, \beta_2) = C_2 \, e^{-\beta_1} e^{-\beta_2} [1 - e^{-\beta_2}]^{K-2} \tag{30}$$

where

$$C_2 = \frac{(K-1)K}{1 - \left(1 - \frac{1}{e}\right)^K} \quad \text{and} \quad K = \frac{U}{T(k_0)}.$$

K is the mean number of fluctuation peaks at $k = k_0$. Using (26) we introduce the new variable $X = X(Y, \beta_1)$ with $Y = \beta_1/\beta_2$. For the distribution function of X we find

$$F(X) = \int_1^\infty d\beta_1 \int_1^X dX' C_2 \frac{\beta_1}{Y^2(X', \beta_1)} \exp\left[-\left(1 + \frac{1}{Y(X', \beta_1)}\right)\beta_1\right] \cdot \left\{1 - \exp\left[-\frac{\beta_1}{Y(X', \beta_1)}\right]\right\}^{K-2} \frac{\partial Y(X', \beta_1)}{\partial X'}.$$

Integrating with respect to X' we obtain

$$F(X) = 1 - C_1 \int_1^\infty d\beta_1 \, e^{-\beta_1} \left\{1 - \exp\left(-\frac{\beta_1}{Y(X, \beta_1)}\right)\right\}^{K-1} \tag{31}$$

with $C_1 = C_2/(K-1)$. The final distribution function for Z is easily obtained by $F(Z) = F[X(Z)]$.

An approximate expression of (31) may be found regarding that the function $Y(X, \beta_1)$ only weakly depends on β_1 in the region where the probability density $p(\beta_1)$ does not vanish. Therefore we set $Y(X, \beta^{max})$ in (31). β^{max} marks the averaged intensity of the highest fluctuation peak at the end of the linear stage, defined by the condition $\bar{N}(U, \beta^{max}) = 1$, cf. (21). Then the distribution function $F(Z)$ is given by

$$F(Z) = 1 - \frac{U}{T(k_0)} Y[X(Z)] \frac{\Gamma\left(\frac{U}{T(k_0)}\right)\Gamma(Y[X(Z)])}{\Gamma\left(\frac{U}{T(k_0)} + Y[X(Z)]\right)}. \tag{32}$$

Γ denotes the gamma function.

In the numerical analysis of these results we denote the second highest pulse as a double pulse if Z lies in the interval $1 \leqq Z < 10$. Then the double-pulse probability is given by $F(Z = 10)$. The numerical comparison of

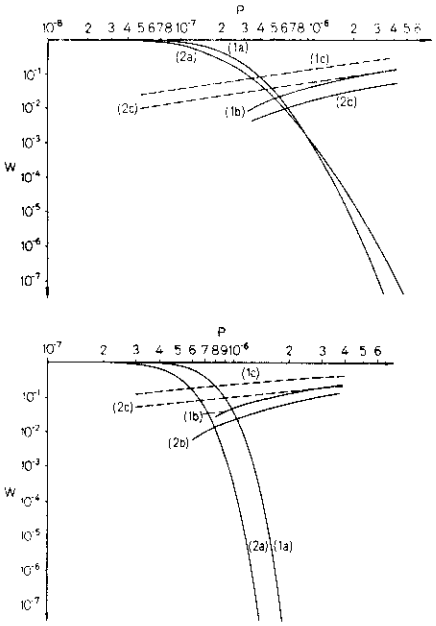

Fig. 2. Breakdown probability (solid lines, index a), double-pulse probability taking into account gain saturation (solid lines, index b), and the double-pulse probability in the model with constant gain (dashed lines, index c) in dependence on the pumping rate P. In curves 1) $a_{Thr} = 0.5$, $\varkappa = 0.3$ and in curves 2) $a_{Thr} = 0.9$, $\varkappa = 0.7$ were used. The cavity round-trip time is $U = 6$ ns. Figure 2a shows the results for ruby laser parameters, Fig. 2b for Nd:glass laser parameters

(31) and (32) shows that the exact formula (31) provides lower double-pulse probabilities than (32). Therefore, the double-pulse probabilities obtained from the approximate formula (32) are upper limits of the exact values. The difference between both formulae sensitively depends on the ratio $\beta^{max}/\beta_D^{max}$ and on $U/T(k_0)$. The error of the approximate equation (32) does not exceed 20% in the region $U/T(k_0) \approx 800$ for $\beta^{max}/\beta_D^{max} \gtrsim 1.5$ and in the region $U/T(k_0) \approx 4000$ for $\beta^{max}/\beta_D^{max} \gtrsim 1.1$. In the region $\beta_D^{max} \approx \beta^{max}$ the approximate distribution function (32) provides a stronger overestimation of the double-pulse probabilities. But this region is characterized by a very high breakdown probability and therefore it is out of interest in experiments.

In the numerical analysis we compare our results with the double-pulse probability derived in the model with

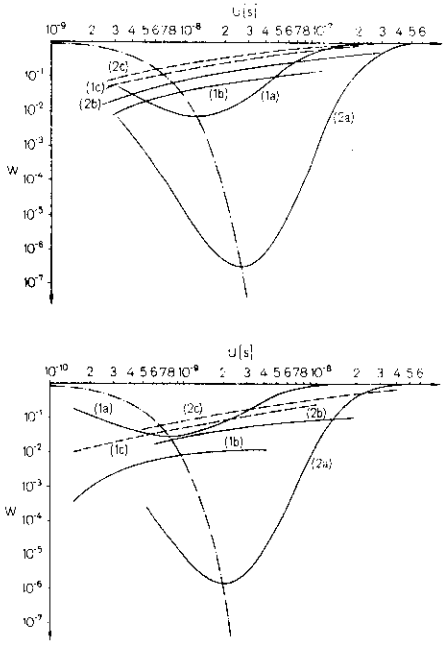

Fig. 3. Breakdown probability (solid lines, index a), double-pulse probability taking into account gain saturation (solid lines, index b), double-pulse probability in the model with constant gain (dashed lines, index c), and position of the minima of the breakdown probability (dash-dot lines) in dependence on the cavity round trip time $U=a_{TW}=0.5$ and $\varkappa=0.3$ were used. Parameter of the curves is $\delta=P/U$. Figure 3a represents the results for the ruby laser for $\delta=100\,s^{-1}$ (curves 1) and $\delta=200\,s^{-1}$ (curves 2). Figure 3b shows the results for the Nd:glass laser for $\delta=100\,s^{-1}$ (curves 1) and $\delta=230\,s^{-1}$ (curves 2)

constant gain during the nonlinear stage by Demokan and Lindsay [5]. In this approximation $Y=Z^{1/s}$ has to be substituted in (32).

Calculating the satellite-pulse probability there should be considered the exact statistics of the intensity maxima. However this would lead to very complicated calculations and does not provide essential corrections of the results [6].

5. Numerical Analysis of the Results

We calculated the breakdown probability (Figs. 2 and 3, solid lines, index a), the double-pulse probability taking into account gain saturation (Figs. 2 and 3, solid lines, index b), and the double-pulse probability in the model with constant gain (Figs. 2 and 3, dashed lines, index c) for Nd:glass and ruby laser parameters, respectively. The parameters used are given in the figure captions. In Fig. 2 the pumping rate P is varied. Comparing the curves (a) and (b) we see that with increasing pumping rate the double-pulse probability changes much slower than the breakdown probability, especially in the Nd:glass system. Corresponding to the experimental claims an optimum pumping rate may be found. The increase of the absorber losses at a fixed value of P leads to a decrease of the double-pulse probability and in the Nd:glass laser also to a decreasing breakdown probability. Figure 2 shows that the ratio of the double-pulse probabilities calculated by using (32) and in the model with constant gain decreases from a factor ten at lower pumping rates to a factor three at higher pumping rates. In Fig. 3 we varied the cavity round trip time U leading to a varying number of fluctuation peaks at the end of the linear stage. Parameter of the curves is $\delta=P/U$. The curves of the breakdown probability are drawn on the left-hand side up to the region where $\beta_D^{\max}\approx 3$, cf. (16). The calculation shows that at a fixed δ a minimum value of the breakdown probability exists. For longer cavities the number of fluctuation peaks at the end of the linear stage increases leading to a faster depletion of the population inversion during the first part of the nonlinear stage. For a short cavity the number of fluctuation peaks at $k=k_0$ is so small that the probability that one of these pulses exceeds the intensity level $\beta_D^{\max}\overline{I(k_0)}$ is small. In both cases the consequence is a higher breakdown probability than at the optimum cavity length. The existence of an optimum cavity length was shown previously by Lariontsev and Serkin [11]. But they did not take into account the important fact that the ratio of the intensity of the highest fluctuation peak to the mean intensity at the end of the linear stage increases with increasing cavity length.

Eliminating δ in the approximate analytical expressions (24) and (25) we can depict the position of the minima of the breakdown probability in Fig. 3 (dash-dot lines). In the experiment shorter cavity round-trip times than U_{opt} may be used in order to obtain an optimum laser regime since the probability of satellite-pulse generation decreases with decreasing cavity length.

In [7] the mean pulse shape and its fluctuations were calculated founded on the model with constant gain during the nonlinear stage. These calculations concerning the highest fluctuation peak keep valid in a good approximation when the intensity of the highest fluctuation peak $\beta^{\max}\overline{I(k_0)}$ at the end of the linear stage exceeds the level $\beta_D^{\max}\overline{I(k_0)}$ by a factor two or more.

References

1. V.S.Letokhov: JETP **55**, 1077 (1968) in Russian
2. P.G.Kryukov, V.S.Letokhov: IEEE J. QE-**8**, 766 (1972)
3. J.A.Fleck, Jr.: Phys. Rev. B **1**, 84 (1970)
4. B.Ya.Zeldovich, T.J.Kusnetzova: Usp. Fiz. Nauk **106**, 47 (1972) in Russian
5. M.S.Demokan, P.A.Lindsay: Int. J. Electron. **41**, 421 (1976)
6. M.S.Demokan, P.A.Lindsay: Int. J. Electron. **42**, 417 (1977)
7. J.Herrmann, F.Weidner: Opt. Quantum Electron. **11**, 119 (1979)
8. S.D.Zakharov, P.G.Kryukov, Yu.A.Matveetz, S.V.Chekalin, O.B.Shatberashvili: Kvantovaya Electron. **5**(17), 52 (1972) in Russian
9. A.N.Zherikin, V.A.Kovalenko, P.G.Kryukov, Yu.A.Matveetz, S.V.Chekalin, O.B.Shatberashvili: Kvantovaya Electron. **1**, 377 (1974) in Russian
10. S.V.Chekalin, P.G.Kryukov, Yu.A.Matveetz, O.B.Shatberashvili: Opto-electronics **6**, 249 (1974)
11. E.G.Lariontsev, V.N.Serkin: Kvantovaya Electron. **1**, 2166 (1974) in Russian
12. W.H.Glenn: IEEE J. QE-**11**, 8 (1975)
13. R.Wilbrandt, H.Weber: IEEE J. QE-**11**, 186 (1975)
14. G.H.C.New: IEEE J. QE-**14**, 642 (1978)
15. D.Middleton: J. Appl. Phys. **19**, 817 (1948)
16. V.I.Tichonov: Usp. Fiz. Nauk **77**, 449 (1961) in Russian